ARTICLES

Analysis of $D^0 \to K\overline{K}X$ decays

D. M. Asner, M. Athanas, D. W. Bliss, W. S. Brower, G. Masek, and H. P. Paar
University of California, San Diego, La Jolla, California 92093

J. Gronberg, C. M. Korte, R. Kutschke, S. Menary, R. J. Morrison, S. Nakanishi, H. N. Nelson, T. K. Nelson, C. Qiao, J. D. Richman, D. Roberts, A. Ryd, H. Tajima, and M. S. Witherell
University of California, Santa Barbara, California 93106

R. Balest, K. Cho, W. T. Ford, M. Lohner, H. Park, P. Rankin, J. Roy, and J. G. Smith
University of Colorado, Boulder, Colorado 80309-0390

J. P. Alexander, C. Bebek, B. E. Berger, K. Berkelman, K. Bloom, D. G. Cassel, H. A. Cho, D. M. Coffman, D. S. Crowcroft, M. Dickson, P. S. Drell, D. J. Dumas, R. Ehrlich, R. Elia, P. Gaidarev, B. Gittelman, S. W. Gray, D. L. Hartill, B. K. Heltsley, C. D. Jones, S. L. Jones, J. Kandaswamy, N. Katayama, P. C. Kim, D. L. Kreinick, T. Lee, Y. Liu, G. S. Ludwig, J. Masui, J. Mevissen, N. B. Mistry, C. R. Ng, E. Nordberg, J. R. Patterson, D. Peterson, D. Riley, A. Soffer, and C. Ward
Cornell University, Ithaca, New York 14853

P. Avery, C. Prescott, S. Yang, and J. Yelton
University of Florida, Gainesville, Florida 32611

G. Brandenburg, R. A. Briere, T. Liu, M. Saulnier, R. Wilson, and H. Yamamoto
Harvard University, Cambridge, Massachusetts 02138

T. E. Browder, F. Li, and J. L. Rodriguez
University of Hawaii at Manoa, Honolulu, Hawaii 96822

T. Bergfeld, B. I. Eisenstein, J. Ernst, G. E. Gladding, G. D. Gollin, M. Palmer, M. Selen, and J. J. Thaler
University of Illinois, Champaign-Urbana, Illinois 61801

K. W. Edwards, K. W. McLean, and M. Ogg
Carleton University, Ottawa, Ontario K1S 5B6
and the Institute of Particle Physics, Canada

A. Bellerive, D. I. Britton, R. Janicek, D. B. MacFarlane, P. M. Patel, and B. Spaan
McGill University, Montréal, Québec H3A 2T8
and the Institute of Particle Physics, Canada

A. J. Sadoff
Ithaca College, Ithaca, New York 14850

R. Ammar, P. Baringer, A. Bean, D. Besson, D. Coppage, N. Copty, R. Davis, N. Hancock, S. Kotov, I. Kravchenko, and N. Kwak
University of Kansas, Lawrence, Kansas 66045

S. Anderson, Y. Kubota, M. Lattery, J. K. Nelson, S. Patton, R. Poling, T. Riehle, and V. Savinov
University of Minnesota, Minneapolis, Minnesota 55455

M. S. Alam, I. J. Kim, Z. Ling, A. H. Mahmood, J. J. O'Neill, H. Severini, C. R. Sun, S. Timm, and F. Wappler
State University of New York at Albany, Albany, New York 12222

J. E. Duboscq, R. Fulton, D. Fujino, K. K. Gan, K. Honscheid, H. Kagan, R. Kass, J. Lee, M. Sung, A. Undrus,* C. White, R. Wanke, A. Wolf, and M. M. Zoeller
Ohio State University, Columbus, Ohio 43210

0556-2821/96/54(7)/4211(10)/$10.00 © 1996 The American Physical Society

X. Fu, B. Nemati, S. J. Richichi, W. R. Ross, P. Skubic, and M. Wood
University of Oklahoma, Norman, Oklahoma 73019

M. Bishai, J. Fast, E. Gerndt, J. W. Hinson, T. Miao, D. H. Miller, M. Modesitt, E. I. Shibata, I. P. J. Shipsey, P. N. Wang, and M. Yurko
Purdue University, West Lafayette, Indiana 47907

L. Gibbons, S. D. Johnson, Y. Kwon, S. Roberts, and E. H. Thorndike
University of Rochester, Rochester, New York 14627

C. P. Jessop, K. Lingel, H. Marsiske, M. L. Perl, S. F. Schaffner, and R. Wang
Stanford Linear Accelerator Center, Stanford University, Stanford, California 94309

T. E. Coan, J. Dominick, V. Fadeyev, I. Korolkov, M. Lambrecht, S. Sanghera, V. Shelkov, R. Stroynowski, I. Volobouev, and G. Wei
Southern Methodist University, Dallas, Texas 75275

M. Artuso, A. Efimov, M. Gao, M. Goldberg, R. Greene, D. He, N. Horwitz, S. Kopp, G. C. Moneti, R. Mountain, Y. Mukhin, S. Playfer, T. Skwarnicki, S. Stone, and X. Xing
Syracuse University, Syracuse, New York 13244

J. Bartelt, S. E. Csorna, V. Jain, and S. Marka
Vanderbilt University, Nashville, Tennessee 37235

A. Freyberger, D. Gibaut, K. Kinoshita, P. Pomianowski, and S. Schrenk
Virginia Polytechnic Institute and State University, Blacksburg, Virginia 24061

D. Cinabro
Wayne State University, Detroit, Michigan 48202

B. Barish, M. Chadha, S. Chan, G. Eigen, J. S. Miller, C. O'Grady, M. Schmidtler, J. Urheim, A. J. Weinstein, and F. Würthwein
California Institute of Technology, Pasadena, California 91125

(CLEO Collaboration)

(Received 16 April 1996)

Using data taken with the CLEO II detector, we have studied the decays of the D^0 to K^+K^-, $K^0\overline{K^0}$, $K_S^0K_S^0K_S^0$, $K_S^0K_S^0\pi^0$, $K^+K^-\pi^0$. We present significantly improved results for $B(D^0\to K^+K^-)=(0.454\pm0.028\pm0.035)\%$, $B(D^0\to K^0\overline{K^0})=(0.054\pm0.012\pm0.010)\%$, and $B(D^0\to K_S^0K_S^0K_S^0)=(0.074\pm0.010\pm0.015)\%$, where the first errors are statistical and the second errors are the estimate of our systematic uncertainty. We also present a new upper limit $B(D^0\to K_S^0K_S^0\pi^0)<0.059\%$ at the 90% confidence level and the first measurement of $B(D^0\to K^+K^-\pi^0)=(0.14\pm0.04)\%$. [S0556-2821(96)00319-0]

PACS number(s): 13.25.Ft, 14.40.Lb

I. INTRODUCTION

Detailed measurements of rare exclusive decay modes of charmed mesons provide a powerful way to probe the details of charmed decays, such as the contributions of W-exchange diagrams and final-state interactions. This allows a probe of the interplay between the weak and strong interactions. The CLEO II experiment is now reaching a level of sensitivity which allows for the systematic study of several rare decay modes of the D^0. In particular, we report the measurements of several decays to final states containing two or more kaons.

A. K^+K^-

This decay mode is Cabibbo suppressed. Some of the Feynman diagrams leading to this final state are shown in Fig. 1. Some years ago it was observed that the ratio $B(D^0\to K^+K^-)/B(D^0\to\pi^+\pi^-)$ was not one. This was surprising since the two decays proceed through similar diagrams. Solutions proposed to explain the deviation from 1 include SU(3) symmetry breaking effects [1], final-state interactions [2–4], and QCD sum rules [5]. A different approach is to invoke penguin diagrams which interfere constructively with the spectator decay for KK but destructively for $\pi\pi$ [6]. The results presented here can be combined with the CLEO II measurement of $D^0\to\pi^+\pi^-$ [7] to give a better measurement of this ratio.

Table I lists a survey of theoretical predictions for the $D^0\to K^+K^-$ branching ratio. The world average for the

*Permanent address: BINP, RU-630090 Novosibirsk, Russia.

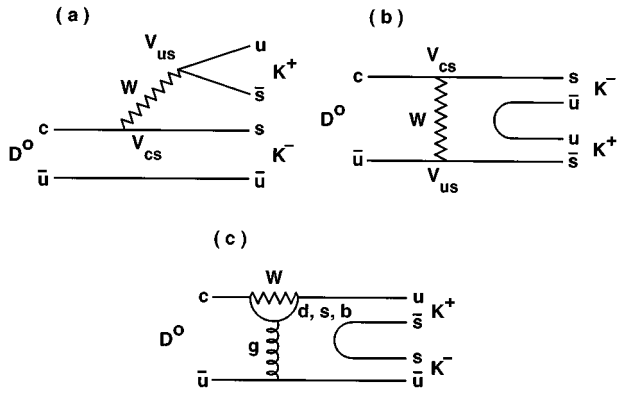

FIG. 1. The most important Feynman diagrams for $D^0 \to K^+K^-$: (a) quark decay, (b) W-exchange decay, and (c) penguins.

branching ratio is $(0.454 \pm 0.029)\%$ [11].

B. $K^0\overline{K^0}$

The $D^0 \to K^0\overline{K^0}$ decay channel allows us to study the effect of final-state interactions. The $D^0 \to K^0\overline{K^0}$ decay is expected to occur primarily via the W-exchange diagrams shown in Fig. 2. Since the Cabibbo factors have opposite signs, we might expect an exact cancellation of the two amplitudes in the four-quark model. In the standard six-quark model the difference between the two amplitudes is tiny, and we thus might expect the branching fraction for the decay to be very small. However, a standard model based calculation predicts a relatively large branching fraction due to final-state rescattering, leading to a branching ratio of $B(D^0 \to K^0\overline{K^0}) = 0.3\%$ [10]. Table I gives a survey of theoretical predictions for the $D^0 \to K^0K^0$ branching ratio. The world average for the branching ratio is $(0.11 \pm 0.04)\%$ [11].

C. $K_S^0K_S^0K_S^0$

Since this decay was first observed by the ARGUS Collaboration $[B(D^0 \to K_S^0K_S^0K_S^0)/B(D^0 \to K^0\pi^+\pi^-) = 0.017 \pm 0.007 \pm 0.005]$ [12], there have been two other measurements, made by CLEO 1.5 $[B(D^0 \to K_S^0K_S^0K_S^0) = (0.11 \pm 0.03)\%]$ [13] and by E687 $[B(D^0 \to K_S^0K_S^0K_S^0)/B(D^0 \to K^0\pi^+\pi^-) = 0.035 \pm 0.012 \pm 0.006]$ [14]. This channel is Cabibbo allowed but the decay does not proceed via a simple spectator process. Instead, its formation requires the popping of an $s\overline{s}$ pair (Fig. 3) and so its existence is an indication of either W-exchange or final-state interactions. We know of no published theoretical predictions for this decay mode.

TABLE I. The present predictions for the KK branching ratios.

Theory models	Branching ratio (%)	
	K^+K^-	$K^0\overline{K^0}$
Spectator model [8]	0.14	0
WSB model [1]	0.56	–
CC model [2]	0.25 ± 0.06	0
FSI model [4]	0.39	0.13
QCD sum rule [5]	0.3	0
K. Terasaki [9]	0.46	0
X. Y. Pham [10]	–	0.3

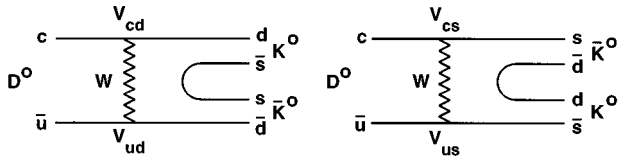

FIG. 2. The Feynman diagrams for $D^0 \to K^0\overline{K^0}$.

D. $K_S^0K_S^0\pi^0$

There has been no previous measurement of this decay rate. This decay channel is Cabibbo suppressed and involves the popping of $d\overline{d}$ or $s\overline{s}$ pairs (Fig. 4). Since the Cabibbo factors have opposite signs between the two amplitudes in each pair, we might expect an almost complete cancellation of the two amplitudes in each pair. We thus might expect the branching fraction for the decay to be very small. We do not distinguish between resonant and nonresonant decay modes. The branching ratio can be compared with that of the Cabibbo favored $K_S^0K_S^0K_S^0$ channel. We know of no published theoretical predictions for this decay mode.

E. $K^+K^-\pi^0$

There has been no previous measurement of this decay rate. This decay is Cabibbo suppressed (Fig. 5). We do not distinguish between resonant and nonresonant decay modes. This result can be compared with the upper limit for the doubly Cabibbo suppressed decay mode of $K^+\pi^-\pi^0$ measured at CLEO II [15]. We know of no published theoretical predictions for this decay mode.

II. ANALYSIS

A. Data sample

We use data taken with the CLEO II detector at the Cornell Electron Storage Ring between November 1990 and July 1993. The data set used in this analysis corresponds to 2.7 fb^{-1} of data taken on and just below the $\Upsilon(4S)$ resonance. For the statistics-limited $K^0\overline{K^0}$ channel, we also use data collected through May 1994, corresponding to an additional 0.8 fb^{-1}.

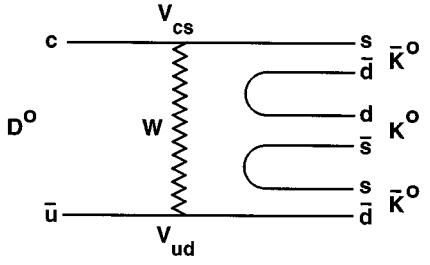

FIG. 3. The Feynman diagram for $D^0 \to K_S^0K_S^0K_S^0$.

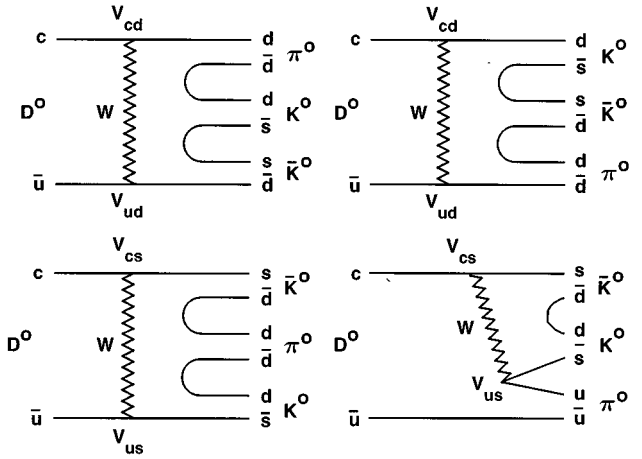

FIG. 4. The most important Feynman diagrams for $D^0 \to K_S^0 K_S^0 \pi^0$.

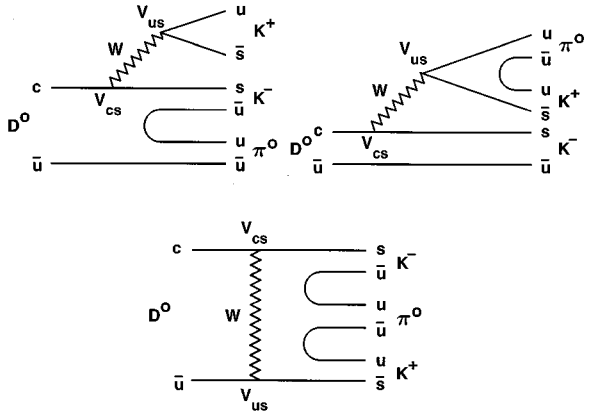

FIG. 5. The most important Feynman diagrams for $D^0 \to K^+ K^- \pi^0$.

The CLEO II detector [16] is designed to detect both charged and neutral particles with excellent resolution and efficiency. The detector consists of a charged particle tracking system surrounded by a time-of-flight (TOF) scintillation system and an electromagnetic shower detector consisting of 7800 thallium-doped cesium iodide crystals. In the ''good barrel'' region, defined as the region where the angle of the shower with respect to the beam axis lies between 45° and 135°, the rms resolution in energy is given by $\delta E/E(\%) = 0.35/E^{0.75} + 1.9 - 0.1E$ (E in GeV). The tracking system, time-of-flight scintillators, and calorimeter are installed inside a 1.5 T superconducting solenoidal magnet. Immediately outside the magnet are iron and chambers for muon detection. The momentum resolution of the tracking system is given by $(\delta p/p)^2 = (0.0015p)^2 + (0.005)^2$, where p is in GeV/c. Ionization loss information (dE/dx) is also provided.

B. Procedure

We use a D^{*+} tag ($D^{*+} \to D^0 \pi^+$ decay mode) for all the channels except the $K_S^0 K_S^0 K_S^0$ channel.[1] Since this latter channel is kinematically restricted, we can see a clean signal without this tag. For the $K^0 \overline{K^0}$ decay channel we add the D^{*0} tag ($D^{*0} \to D^0 \pi^0$ decay mode) so as to increase the number of events, even though the mass difference resolution for the D^{*0} tag is not as good as that for the D^{*+} tag. Table II summarizes the tags and normalization modes used. To get the Monte Carlo (MC) efficiencies, we generated 20 000 events in each channel. In this analysis, we will assume that the D^0 and $\overline{D^0}$ partial decay rates are equal since an inequality could only result if the processes were CP violating. An earlier analysis shows that any CP asymmetries are small [17]. The following analyses sum both charges.

C. The initial selection

We first reconstruct the D^0 decay mode of interest. Details of this reconstruction can be found in the sections on each specific decay mode. The D^0 candidate is then combined with a pion to reconstruct a $D^{*+} \to D^0 \pi^+$ candidate. This pion is denoted as the soft pion. In this reconstruction, the dominant source of background is combinatorics − random combinations of tracks which accidentally give the expected mass. This background is mostly due to either a correctly reconstructed D^0 which is combined with a wrong soft pion, or a fake D^0 in which at least one of the decay products is misidentified, combined with the correct soft pion from the D^* decay.

We select D^*'s by requiring that the reconstructed mass difference $\Delta M (\equiv M_{D^{*+}} - M_{D^0})$ lies within 2.0 MeV/c^2 ($\sim 3\sigma$) of the nominal mass difference of 145.4 MeV/c^2. This cut strongly suppresses the background coming from random combinations of tracks which accidentally give the expected masses.

Most of the background comes from using a wrong soft pion to form the D^*. We determine the number of these events by fitting the ΔM background distribution and integrating under the curve in the signal region. The functional form used is

$$a(\Delta M - m_{\pi^+})^{0.5} + b(\Delta M - m_{\pi^+})^{1.5} + c(\Delta M - m_{\pi^+})^{2.5},$$

where m_{π^+} is π^+ mass, the first term is from a nonrelativistic model of phase space, and the second and third terms are the first- and second-order relativistic corrections to the nonrelativistic model, respectively.

The momentum spectrum for continuum charm production is peaked at large momentum, while that for the combinatoric background, from both continuum and B decay, is peaked at low D^* momentum. D^* candidates are therefore

TABLE II. Tags and normalization modes.

Channel	Tag	Normalization mode
K^+K^-	$D^{*\pm}$	$K^-\pi^+$
$K^0\overline{K^0}$	$D^{*\pm}, D^{*0}$	$\overline{K^0}\pi^+\pi^-$
$K_S^0K_S^0K_S^0$	No tag	$\overline{K^0}\pi^+\pi^-$
$K_S^0K_S^0\pi^0$	$D^{*\pm}$	$\overline{K^0}\pi^+\pi^-$
$K^+K^-\pi^0$	$D^{*\pm}$	$K^-\pi^+\pi^0$

[1]Throughout this paper, any reference to a specific decay or state also implies a reference to its charge conjugate.

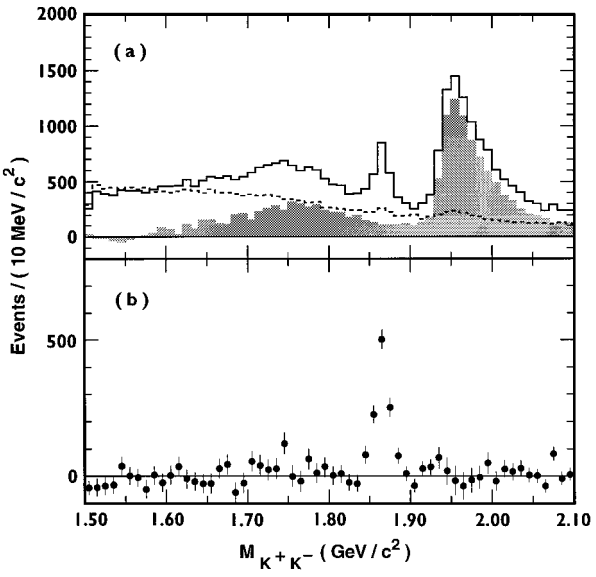

FIG. 6. (a) The K^+K^- invariant mass distribution. The solid line is the D^0 mass signal in the mass difference signal region. The dotted line is the background from the mass difference sideband region. The shaded area represents the background coming from other charm decay modes after doing the ΔM sideband subtraction. This background is determined by Monte Carlo events. We see a peak around 1.98 GeV/c^2 due to misidentified $D^0 \to K^-\pi^+$ events. (b) The reconstructed K^+K^- invariant mass distribution after subtracting all the backgrounds.

required to have a momentum (p) greater than 2.45 GeV/c which is equivalent to a cut of x_p greater than 0.5, where $x_p = p/p_{\max}$ with $p_{\max} = \sqrt{E^2_{\rm beam} - m^2_{D*}}$. This means that we exclude charm events coming from B decays.

We detect π^0's by their decays to $\gamma\gamma$. Candidate π^0's are formed by taking two-photon combinations. The individual photons appear as clusters in the CsI calorimeter. The energy of each cluster has to be at least 30 MeV and the diphoton combination must have at least one photon in the higher resolution portion of the calorimeter [$|\cos(\theta)| < 0.71$, where θ is the angle with respect to the beam axis]. We reject all clusters matched to charged tracks in the central detector. We require that the momentum of the diphoton combination be greater than 0.2 GeV/c and that the mass of this combination be within $3\sigma(\sim 15$ MeV/c^2) of the nominal pion mass.

When we did a systematic check of the effects of our event selection cuts, we compared and corrected the D^* momentum distribution between real data and MC using the normalization mode of $D^0 \to K^-\pi^+$ to ensure that we had the same momentum distribution for both samples. Then, we checked the effect of varying the D^* momentum cut.

III. MEASUREMENTS AND RESULTS

A. K^+K^-

For this channel we apply a cut on the kaon momentum of $P_{K^\pm} > 0.3$ GeV/c, and require that $|\cos\theta_{K^\pm}| < 0.8$ where the angle $\theta_{K^\pm}$ is the angle between the $K^\pm$ momentum in the D^0 rest frame and the D^0 laboratory momentum. Since the D^0, K^+, and K^- are spinless particles, the D^0 decays isotropically, whereas the background shows a peak at $|\cos\theta_{K^\pm}| \approx 1.0$.

Using these cuts, we obtain the D^0 mass spectrum shown in Fig. 6(a). For this channel the signal region is between 1.84 and 1.89 GeV/c^2. The D^0 signal region is defined to be within 3σ of the fitted mass, determined using a Gaussian fit of the real data. The number of events in the D^0 signal region is 2785 and the number of background events coming from the mass difference sideband region is 1119 ± 20 where the error comes from statistics in the sideband regions, which determine the background normalization. Since we determine these numbers by scaling the ΔM sideband contributions, the error is smaller than the square root of the number of events. We also consider the statistical uncertainty in the ΔM background shape as a systematic error.

At this stage, there is the possibility that backgrounds from other charm decay modes such as $K^-\pi^+\pi^0$ are also present in the D^0 signal region even if most of these events lie outside it. To determine this background, we use a MC simulation of continuum charmed hadron production and decay based on JETSET 7.3, followed by a full GEANT-based simulation of the signals that the particles produce in the detector. We treat these events as data and do the ΔM sideband subtraction. The result is given in Fig. 6(a). The normalization of the simulated events is absolutely determined from the luminosity. We find 564 ± 40 background events from this source. After subtracting all the backgrounds, we find $N(K^+K^-) = 1102 \pm 69$ for $D^0 \to K^+K^-$. In order to show how well the backgrounds are understood, the background contributions to Fig. 6(a) have been subtracted from the data (solid line) histogram and the result is shown in Fig. 6(b). This subtracted histogram was not used to calculate the yields and is included purely for illustrative purposes. For this decay mode, one advantage of the above procedure, compared with simply fitting the K^+K^- mass plot, is that it avoids the necessity of fitting the complicated background shape which arises from the misidentification of other D^0 decay modes.

To get the branching ratio, we use $D^0 \to K^-\pi^+$ as the normalization mode

$$\frac{B(D^0 \to K^+K^-)}{B(D^0 \to K^-\pi^+)} = \left[\frac{N(K^+K^-)}{\epsilon_{K^+K^-}}\right]\left[\frac{\epsilon_{K^-\pi^+}}{N(K^-\pi^+)}\right],$$

where N is the number of observed events in each case and ϵ is the corresponding reconstruction efficiency which includes the D^{*+} reconstruction efficiency as determined from MC events. The detector efficiencies from MC simulation are $\epsilon_{K^+K^-} = (22.9 \pm 0.3)\%$ and $\epsilon_{K^-\pi^+} = (37.7 \pm 0.5)\%$. We observe $N(K^-\pi^+) = 15\,633 \pm 202$ for $D^0 \to K^-\pi^+$. We measure $B(D^0 \to K^+K^-)/B(D^0 \to K^-\pi^+) = 0.116 \pm 0.007$.

As a systematic check of the effect of our event selection cuts, we extract the signal yields with the mass difference cut, D^* momentum cut, and the decay angle cut individually tightened by 20% of their nominal values. We take the largest effect on the yield as setting the size of the systematic error, giving a contribution to the systematic error of 2.0%. The systematic error, due to the statistical uncertainty in the ΔM background functional form used to get the number of background events coming from the mass difference side-

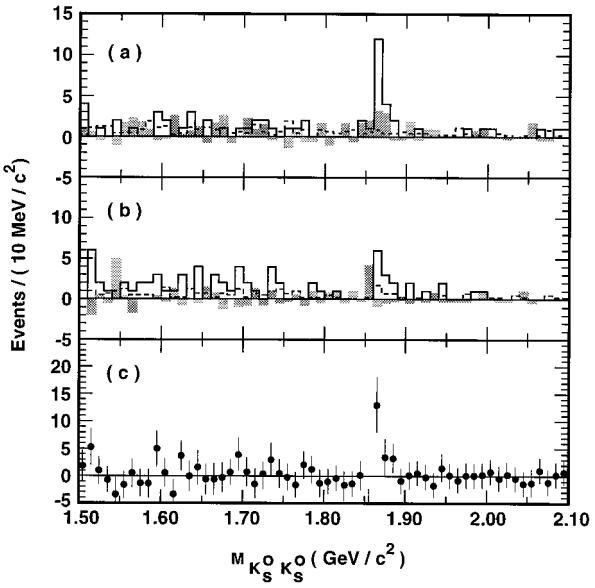

FIG. 7. (a) The invariant mass distribution for $K^0_S K^0_S$ for the $D^{*\pm}$ tag. (b) The invariant mass distribution for $K^0_S K^0_S$ for the D^{*0} tag. The solid line is the D^0 mass signal in the mass difference signal region. The dotted line is background from the mass difference sideband region. The shaded area represents the background coming from other charm decay modes after doing the mass difference sideband subtraction. This background is determined by Monte Carlo events. (c) The sum of the invariant mass distribution for $K^0_S K^0_S$ for $D^{*\pm}$ tag and D^{*0} tag data after subtracting all the backgrounds.

band region, is 5.3%. The variations of the yield with different sideband subtractions and different fitting methods are negligible compared to the other systematic errors. The systematic error due to limited MC statistics is 2.0%. This gives a total systematic error of 6.0%. Using $B(D^0 \to K^- \pi^+) = (3.91 \pm 0.08 \pm 0.17)\%$ [18], we measure $B(D^0 \to K^+ K^-) = (0.454 \pm 0.028 \pm 0.035)\%$.

B. $K^0 \overline{K^0}$

We study the $K^0_S K^0_S$ component of this decay. Because of the small number of events, we use both the $D^{*\pm}$ tag and the D^{*0} tag.

In this channel the dominant sources of backgrounds are from nonresonant $K^0_S \pi^+ \pi^-$ and $\pi^+ \pi^- \pi^+ \pi^-$ production. To reduce feedthrough from $D^0 \to K^0_S \pi^+ \pi^-$, where the $\pi^+ \pi^-$ fakes a K^0_S or from $D^0 \to \pi^+ \pi^- \pi^+ \pi^-$, where the four pions fake 2 K^0_S's, we first reconstruct K^0_S mesons from $\pi^+ \pi^-$ pairs with an invariant mass within 0.0108 GeV/c^2 ($\sim 3\sigma$) of the nominal K^0_S mass and a vertex displaced at least 5 mm from the beam position. We also apply a $|\cos_{\theta_{K^0_S}}| < 0.8$ cut, where the angle $\theta_{K^0_S}$ is the angle between the K^0_S momentum in the D^0 rest frame and the D^0 laboratory momentum.

To get the branching ratio, we use

TABLE III. Summary of systematic errors for the $K^0 \overline{K^0}$ channel.

Source of error	Systematic errors (%) $D^{*\pm}$ tag	D^{*0} tag
Uncorrelated error	18.2	15.6
Signal yield (cuts)	(17.4)	(12.5)
Nonresonant $\pi^+ \pi^-$ background	(3.8)	(0.0)
MC statistics	(3.5)	(9.4)
Correlated error	5.0	5.0
K^0_S's finding efficiency	(5.0)	(5.0)
Total	18.9	16.4

$$\frac{B(D^0 \to K^0 \overline{K^0})}{B(D^0 \to \overline{K^0} \pi^+ \pi^-)} = \frac{1}{B(K^0_S \to \pi^+ \pi^-)} \left[\frac{N(K^0_S K^0_S)}{\epsilon_{K^0_S K^0_S}} \right] \left[\frac{\epsilon_{K^0_S \pi^+ \pi^-}}{N(K^0_S \pi^+ \pi^-)} \right],$$

where N is the number of observed events in each case and ϵ is the corresponding reconstruction efficiency. Because $B(D^0 \to K^0 \overline{K^0}) = 2B(D^0 \to K^0_S K^0_S)$ ($D^0 \to K^0_S K^0_L$ is forbidden) [19], the factors $B(\overline{K^0} \pi^+ \pi^- \to K^0_S \pi^+ \pi^-)$ and $B(K^0 \overline{K^0} \to K^0_S K^0_S)$ become equal and cancel in the above equation [20]. We use $B(K^0_S \to \pi^+ \pi^-) = (68.6 \pm 0.3)\%$ [11]. The yield was extracted in the same way as for the $K^+ K^-$ channel.

1. $D^{*\pm}$ tag

Using the $D^{*\pm}$ tag, we obtain the D^0 mass spectrum shown in Fig. 7(a). For this tag the signal region is between 1.84 and 1.89 GeV/c^2. The number of events in the D^0 signal region is 21 and the number of background events coming from the mass difference sideband region is 2.8 ± 0.8, yielding $N(K^0_S K^0_S) = 18.2 \pm 4.6$. At this stage, in order to check the background from other charm decay modes, we run on Monte Carlo events using the same cuts as for the $K^0 \overline{K^0}$ channel. We find that the background comes from the nonresonant $\pi^+ \pi^-$ decay modes such as $K^0_S \pi^+ \pi^-$ and $\pi^+ \pi^- \pi^+ \pi^-$ and therefore is calculated using the sideband method. Since real data are more reliable and have a smaller associated statistical error than the Monte Carlo events, we use only the real data for background subtraction and use the sideband region of the K^0_S mass domain to determine the nonresonant $\pi^+ \pi^-$ background. We consider this background to be a source of a systematic error. The detection efficiencies determined by MC simulation are $\epsilon_{K^0_S K^0_S} = (8.4 \pm 0.2)\%$ and $\epsilon_{K^0_S \pi^+ \pi^-} = (13.4 \pm 0.3)\%$. We get $N(K^0_S \pi^+ \pi^-) = 4470 \pm 137$, giving $B(D^0 \to K^0 \overline{K^0})/B(D^0 \to \overline{K^0} \pi^+ \pi^-) = 0.0094 \pm 0.0024$ for this tag.

2. D^{*0} tag

We use a more restrictive mass difference cut $|M_{D^{*0}} - M_{D^0} - 0.1423| < 0.0022$ GeV/c^2 ($\sim 2.5\sigma$) for the

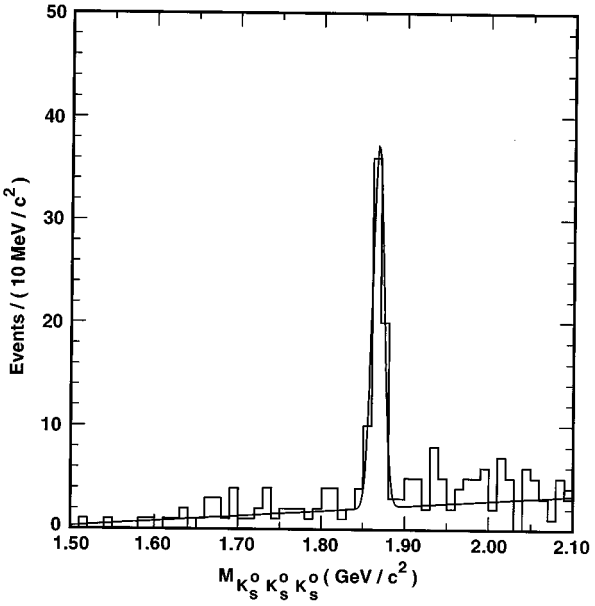

FIG. 8. The invariant mass distribution of $K_S^0K_S^0K_S^0$ The signal is fitted using a Gaussian while the background is fit to a straight line.

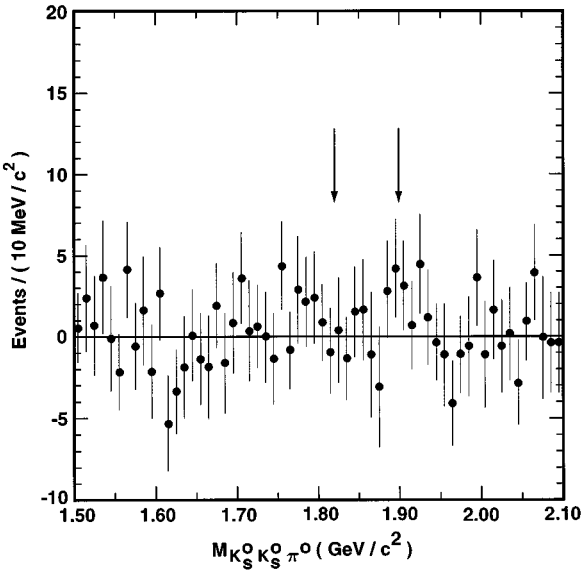

FIG. 9. The invariant mass distribution of $K_S^0K_S^0\pi^0$ after subtracting all the backgrounds. The arrows show the signal region.

D^{*0} tag since the resolution of the mass difference is poorer for this channel. We obtain the D^0 mass spectrum shown in Fig. 7(b). For this tag the signal region lies between 1.84 and 1.89 GeV/c^2. The number of events in the D^0 signal region is 11 and the number of background events coming from the mass difference sideband region is 3.4 ± 0.8. This gives $N(K_S^0K_S^0)=7.6\pm3.4$ after background subtraction. The detection efficiencies determined from MC are $\epsilon_{K_S^0K_S^0}=(3.5\pm0.2)\%$ and $\epsilon_{K_S^0\pi^+\pi^-}=(6.8\pm0.6)\%$. We get $N(K_S^0\pi^+\pi^-)=1589\pm71$, and we measure $B(D^0\to K^0\overline{K^0})/B(D^0\to\overline{K^0}\pi^+\pi^-)=0.0134\pm0.0060$ for this tag.

Figure 7(c) shows the sum of the $D^{*\pm}$ tag and the D^{*0} tag data after subtracting all the backgrounds. As a systematic check of the effect of our event selection cuts, we extract the signal yields with the mass difference cut, D^* momentum cut, the decay angle cut, the vertex cut, and the K_S^0 mass cut individually tightened by 20% of their nominal values. We take the largest effect on the yield as setting the size of the systematic error. Another systematic error is due to the possibility that backgrounds from other charm decay modes such as $K^0\pi^+\pi^-$ or $\pi^+\pi^-\pi^+\pi^-$ are also present in the D^0 signal region. In order to check this, we studied a sideband region in the K_S^0's mass domain to determine the nonresonant $\pi^+\pi^-$ background. Results indicate that there are 0.7 nonresonant $\pi^+\pi^-$ background events in D^0 signal region for the $D^{*\pm}$ tag and none for the D^{*0} tag. The other systematic error is the uncertainty in the K_S^0 finding efficiency. We get this systematic error by comparing K_S^0 yields (reconstructed via the $\pi^+\pi^-$ mode) when using the K_S^0 finding subroutine and when using the same routine with some cuts relaxed. This error on this efficiency is 5% per K_S^0 which does not include track systematic error. The track-finding efficiency of K_S^0 daughters is cancelled by that of the normalization mode. The error on the K_S^0 finding efficiency gives a correlated systematic error affecting both $D^{*\pm}$ and D^{*0} tags. All the other systematic errors are uncorrelated. A summary of the systematic errors for this channel is given in Table III.

The final ratios of $B(D^0\to K^0\overline{K^0})/B(D^0\to\overline{K^0}\pi^+\pi^-)$ are $0.0094\pm0.0024\pm0.0017\pm0.0005$ for the $D^{*\pm}$ tag and $0.0134\pm0.0060\pm0.0021\pm0.0007$ for the D^{*0} tag where the first errors are statistical, the second are the uncorrelated systematic errors and the last are the correlated systematic errors. Finally, we combine the data from the two tags. The combined ratio is $B(D^0\to K^0\overline{K^0})/B(D^0\to\overline{K^0}\pi^+\pi^-)=0.0101\pm0.0022(\text{stat})\pm0.0016(\text{syst})$. Using $B(D^0\to K^0\pi^+\pi^-)=(5.3\pm0.6)\%$ [11], we obtain $B(D^0\to K^0K^0)=[0.054\pm0.012(\text{stat})\pm0.010(\text{syst})]\%$.

C. $K_S^0K_S^0K_S^0$

This particular mode is essentially background free due to its kinematics, so we do not require a D^* tag. Three K_S^0's have to be observed, which makes the efficiency rather low, so the K_S^0 cuts used for this decay are looser than those we use for the other analyses described in this paper.

We first reconstruct K_S^0 mesons from $\pi^+\pi^-$ pairs with an invariant mass within 0.0108 GeV/c^2($\sim3\sigma$) of the nominal K_S^0 mass and a vertex displaced at least 2 mm from the beam position. We plot the $K_S^0K_S^0K_S^0$ invariant mass for $P_{D^0}>2.48$ GeV/c which is similar to requiring x_p greater than 0.5. For this mode, we have to use the fitting method. We do not use a D^{*+} tag and therefore we do not do a mass difference sideband subtraction. This $K_S^0K_S^0K_S^0$ invariant mass distribution is fitted using a Gaussian and Chebyshev polynomial of order 1. We obtain a signal of $N(K_S^0K_S^0K_S^0)=61.0\pm8.4$ (Fig. 8).

To get the branching ratio, we use

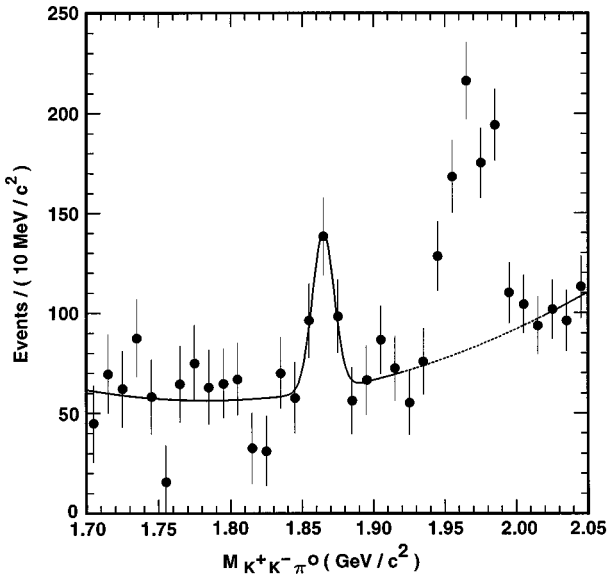

FIG. 10. The invariant mass distribution of $K^+K^-\pi^0$ after doing the normalized mass difference sideband subtraction. In fitting, we exclude the region between 1.92 and 2.02 GeV/c^2 due to an excess of misidentified $D^0\to K^-\pi^+\pi^0$ events which survive the veto.

$$\frac{B(D^0\to K_S^0K_S^0K_S^0)}{B(D^0\to \overline{K^0}\pi^+\pi^-)} = \frac{1}{B(K_S^0\to\pi^+\pi^-)^2}\left[\frac{N(K_S^0K_S^0K_S^0)}{\epsilon_{K_S^0K_S^0K_S^0}}\right]\left[\frac{\epsilon_{K_S^0\pi^+\pi^-}}{2N(K_S^0\pi^+\pi^-)}\right],$$

where N is the number of observed events in each case and ϵ is the corresponding reconstruction efficiency. The detection efficiencies determined from MC simulation are $\epsilon_{K_S^0K_S^0K_S^0}=(5.2\pm0.2)\%$ and $\epsilon_{K_S^0\pi^+\pi^-}=(16.8\pm0.4)\%$. We get $N(K_S^0\pi^+\pi^-)=14\,993\pm457$. Using $B(K_S^0\to\pi^+\pi^-)=(68.6\pm0.3)\%$ [11], we measure $B(D^0\to K_S^0K_S^0K_S^0)/B(D^0\to\overline{K^0}\pi^+\pi^-)=0.0139\pm0.0019$.

As a systematic check, we study the variations of the yield with the D^0 momentum cut, the vertex cut and the K_S^0 mass cut individually tightened by 20% of their nominal values. The biggest systematic error due to these cut variations is 13.5%. The systematic error due to the K_S^0 finding efficiency for two K_S^0 in the CLEO II detector is 10.0%. The systematic error due to the MC statistics is 3.9%. So, the total systematic error is 17.2%. Finally, using $B(D^0\to\overline{K^0}\pi^+\pi^-)=(5.3\pm0.6)\%$ [11], we measure $B(D^0\to K_S^0K_S^0K_S^0)=[0.074\pm0.010(\text{stat})\pm0.015(\text{syst})]\%$.

D. $K_S^0K_S^0\pi^0$

In this decay mode, there are very few events and the background is large. So, we use the same tight cuts on the K_S^0's as we do for the $K_S^0K_S^0$ channel.

For this channel the signal region is between 1.82 and 1.90 GeV/c^2. The number of events in the signal region is 35 and the number of background events, estimated using the mass difference sidebands, is 24 ± 2. Using the same methods as for the K^+K^- channel, we find from Monte Carlo simulation that other charm decay modes contribute 6 ± 6 events to the signal region. After subtracting all the backgrounds (Fig. 9), we get $N(K_S^0K_S^0\pi^0)=5\pm9$. The corresponding unsubtracted figures are omitted. The signal is consistent with zero. We therefore calculate an upper limit on the branching fraction.

To get the branching ratio, we use

$$\frac{B(D^0\to K_S^0K_S^0\pi^0)}{B(D^0\to\overline{K^0}\pi^+\pi^-)} = \frac{1}{B(K_S^0\to\pi^+\pi^-)}\left[\frac{N(K_S^0K_S^0\pi^0)}{\epsilon_{K_S^0K_S^0\pi^0}}\right]\left[\frac{\epsilon_{K_S^0\pi^+\pi^-}}{2N(K_S^0\pi^+\pi^-)}\right],$$

where N is the number of the observed events in each case and ϵ is the corresponding reconstruction efficiency. The detection efficiencies determined from MC simulation are $\epsilon_{K_S^0K_S^0\pi^0}=(5.3\pm0.2)\%$ and $\epsilon_{K_S^0\pi^+\pi^-}=(13.4\pm0.3)\%$. All the systematic errors are negligible given the size of the statistical error and so have not been included. We get $N(K_S^0\pi^+\pi^-)=3184\pm102$. Using $B(K_S^0\to\pi^+\pi^-)=(68.6\pm0.3)\%$, we get $B(D^0\to K_S^0K_S^0\pi^0)/B(D^0\to\overline{K^0}\pi^+\pi^-)=0.0029\pm0.0052$. Using $B(D^0\to\overline{K^0}\pi^+\pi^-)=(5.3$

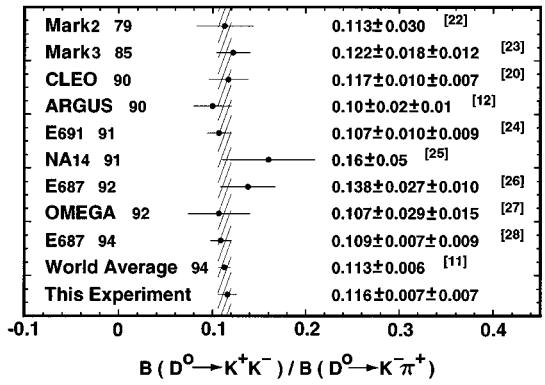

FIG. 11. The previous measurements and our result for the $B(D^0\to K^+K^-)/B(D^0\to K^-\pi^+)$ ratio. The hatched area indicates the world average.

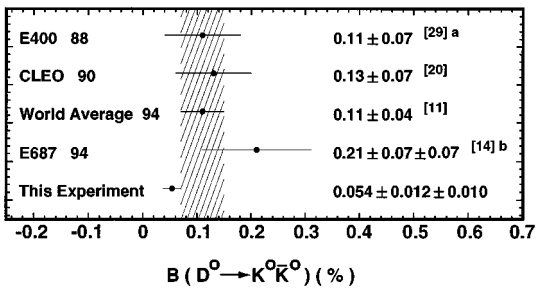

FIG. 12. The previous measurements and our result for the $B(D^0\to K^0\bar{K}^0)$ channel. The hatched area indicates the world average. (a) We have used $B(D^0\to K^+K^-)=(0.454\pm0.029)\%$ [11]. (b) We have used $B(D^0\to\overline{K^0}\pi^+\pi^-)=(5.3\pm0.6)\%$ [11].

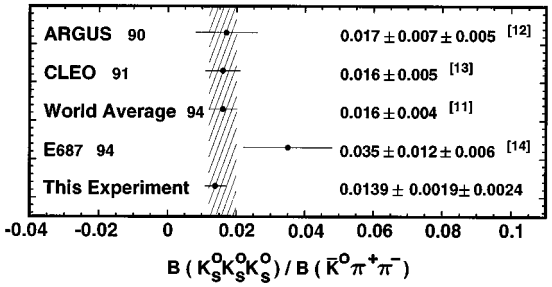

FIG. 13. The previous measurements for $B(D^0 \to K_S^0 K_S^0 K_S^0)/B(D^0 \to \overline{K^0}\pi^+\pi^-)$ and our result for this ratio. The hatched area indicates the world average.

$\pm 0.6)\%$ [11], we measure $B(D^0 \to K_S^0 K_S^0 \pi^0) = (0.015 \pm 0.027)\%$ or $B(D^0 \to K_S^0 K_S^0 \pi^0) < 0.059\%$ at the 90% confidence level.

E. $K^+K^-\pi^0$

Finally, we measure $D^0 \to K^+K^-\pi^0$. For this decay mode, the misidentification of a π^+ as a K^+ is the largest source of background. The major source of this background is from the decay $D^{*+} \to D^0\pi^+$ followed by the Cabibbo favored decay $D^0 \to K^-\pi^+\pi^0$. Since the branching ratio $B(D^0 \to K^-\pi^+\pi^0)$ for this background is much bigger than the branching ratio $B(D^0 \to K^-\pi^+)$ for the K^+K^- channel background $(B(D^0 \to K^-\pi^+\pi^0)/B(D^0 \to K^-\pi^+) = 3.78 \pm 0.071$ [21]), we use tighter cuts than those for the K^+K^- channel.

In order to select the $K^+K^-\pi^0$ decay mode and reduce the $K^-\pi^+\pi^0$ background, we change a kaon candidate track assignment to a pion candidate track and calculate the resultant D^0 mass ($M_{K^-\pi^+\pi^0}$). If $M_{K^-\pi^+\pi^0}$ is within 3σ of the nominal D^0 mass, we eliminate the combination. We also use a tight cut $P_{D^{*+}} > 2.93$ GeV/c which is equivalent to requiring x_p greater than 0.6.

We require that the normalized difference between the expected and measured dE/dx for the kaon hypothesis be within 2σ for both kaons. We also require $P_{K^\pm} > 0.3$ GeV/c. We use the same π^0 selection described in Sec. II C except for requiring that the momentum of the π^0 be greater than 0.4 GeV/c and that the mass of the π^0 be within $2\sigma(\sim 10$ MeV/c^2) of the nominal pion mass.

Using these cuts, we obtain the D^0 mass spectrum shown in Fig. 10 after doing the normalized mass difference sideband subtraction. For this mode, we have to use the fitting method since the backgrounds from other charm decay modes are so complicated that the fitting method is more reliable. It is fitted by a Gaussian and a Chebyshev polynomial of order 2. We get a signal of $N(K^+K^-\pi^0) = 151 \pm 42$, and $\epsilon_{K^+K^-\pi^0} = (9.2 \pm 0.3)\%$.

TABLE IV. Summary of the branching fractions, where the first error is statistical and the second is the estimate of our systematic uncertainty.

Channel	Theory (%)	B (%)	World average (%)
K^+K^-	0.14–0.56	$0.454 \pm 0.028 \pm 0.035$	0.454 ± 0.029
$K^0\overline{K^0}$	0–0.3	$0.054 \pm 0.012 \pm 0.010$	0.11 ± 0.04
$K_S^0K_S^0K_S^0$		$0.074 \pm 0.010 \pm 0.015$	0.086 ± 0.025
$K_S^0K_S^0\pi^0$		< 0.059 @90% CL	
$K^+K^-\pi^0$		0.14 ± 0.04	

To get the branching ratio, we use

$$\frac{B(D^0 \to K^+K^-\pi^0)}{B(D^0 \to K^-\pi^+\pi^0)} = \left[\frac{N(K^+K^-\pi^0)}{\epsilon_{K^+K^-\pi^0}}\right]\left[\frac{\epsilon_{K^-\pi^+\pi^0}}{N(K^-\pi^+\pi^0)}\right].$$

We get $\epsilon_{K^-\pi^+\pi^0} = (4.7 \pm 0.3)\%$ and $N(K^-\pi^+\pi^0) = 8151 \pm 246$, giving the ratio $B(D^0 \to K^+K^-\pi^0)/B(D^0 \to K^-\pi^+\pi^0) = 0.0095 \pm 0.0026$. Using the ratio $B(D^0 \to K^-\pi^+\pi^0)/B(D^0 \to K^-\pi^+) = 3.78 \pm 0.071$ [21] and $B(D^0 \to K^-\pi^+) = (3.91 \pm 0.08 \pm 0.17)\%$ [18], we get $B(D^0 \to K^+K^-\pi^0) = (0.14 \pm 0.04)\%$. All the other systematic errors are negligible given the size of the statistical error.

IV. SUMMARY AND CONCLUSIONS

We have investigated D^0 decays to several rare final states which have two or three kaons in the final state. Figures 11 [22–28], 12 [29], and 13 show the previous measurements and our results for K^+K^-, $K^0\overline{K^0}$, and $K_S^0K_S^0K_S^0$, respectively. Table IV gives the final summary of our results, where the first error is statistical and the second is the estimate of our systematic uncertainty. The K^+K^-, $K^0\overline{K^0}$, and $K_S^0K_S^0K_S^0$ results have significantly smaller errors than earlier measurements. We also report the first upper limit on the $D^0 \to K_S^0K_S^0\pi^0$ branching fraction and the first measurement of the $D^0 \to K^+K^-\pi^0$ branching fraction.

ACKNOWLEDGMENTS

We gratefully acknowledge the efforts of the CESR staff in providing us with excellent luminosity and running conditions. J.P.A., J.R.P., and I.P.J.S. thank the NYI program of the NSF, M.S. thanks the PFF program of the NSF, G.E. thanks the Heisenberg Foundation, K.K.G., M.S., H.N.N., T.S., and H.Y. thank the OJI program of DOE, J.R.P, K.H., and M.S. thank the A.P. Sloan Foundation, and A.W. and R.W. thank the Alexander von Humboldt Stiftung for support. This work was supported by the National Science Foundation, the U.S. Department of Energy, and the Natural Sciences and Engineering Research Council of Canada.

[1] M. Bauer *et al.*, Z. Phys. C **34**, 103 (1987).
[2] L. L. Chau, Phys. Rep. **95**, 1 (1983).
[3] A. N. Kamal *et al.*, Phys. Rev. D **35**, 3515 (1987); **36**, 3510 (1987); L. L. Chau *et al.*, Phys. Lett. B **280**, 281 (1992).
[4] A. Czarnecki *et al.*, Z. Phys. C **54**, 411 (1992).
[5] B. Yu and M. Shifman, Sov. J. Nucl. Phys. **45**, 522 (1987).
[6] M. Gluck, Phys. Lett. **88B**, 145 (1979); J. Finjord, Nucl. Phys. **B181**, 74 (1981).

[7] CLEO Collaboration, M. Selen *et al.*, Phys. Rev. Lett. **71**, 1973 (1993).
[8] N. Cabibbo and L. Maiani, Phys. Lett. **73B**, 418 (1978).
[9] K. Terasaki and S. Oneda, Phys. Rev. D **38**, 132 (1988).
[10] X. Y. Pham, Phys. Lett. B **193**, 331 (1987).
[11] Particle Data Group, L. Montanet *et al.*, Phys. Rev. D **50**, 1173 (1994).
[12] ARGUS Collaboration, H. Albrecht *et al.*, Z. Phys. C **46**, 9 (1990).
[13] CLEO Collaboration, R. Ammar *et al.*, Phys. Rev. D **44**, 3383 (1991).
[14] E687 Collaboration, P. L. Frabetti *et al.*, Phys. Lett. B **340**, 254 (1994).
[15] CLEO Collaboration, G. Crawford *et al.*, in *Proceedings of the 27th International Conference on High Energy Physics*, Glasgow, Scotland, 1994, edited by P. J. Bussey and I. G. Knowles (IOP, London, 1995).
[16] CLEO Collaboration, Y. Kubota *et al.*, Nucl. Instrum. Methods Phys. Res. A **320**, 66 (1992).
[17] CLEO Collaboration, J. Bartelt *et al.*, Phys. Rev. D **52**, 4860 (1995).
[18] CLEO Collaboration, D. S. Akerib *et al.*, Phys. Rev. Lett. **71**, 3070 (1993).
[19] This factor could differ from two if other diagrams contributed to the decay and interfered. CP violation allows for the possibility that the D^0 can decay to $K_S^0 K_L^0$. However, we assume that any such contributions would be small and can safely be neglected.
[20] CLEO Collaboration, J. Alexander *et al.*, Phys. Rev. Lett. **65**, 1184 (1990).
[21] CLEO Collaboration, L. Gibbons *et al.*, Report No. EPS0179, Report No. CLEO CONF95-18, 1995 (unpublished).
[22] Mark 2 Collaboration, G. S. Abrams *et al.*, Phys. Rev. Lett. **43**, 481 (1979).
[23] Mark 3 Collaboration, R. M. Baltrusaitis *et al.*, Phys. Rev. Lett. **55**, 150 (1985).
[24] E691 Collaboration, J. C. Anjos *et al.*, Phys. Rev. D **44**, R3371 (1991).
[25] NA14 Collaboration, M. P. Alvarez *et al.*, Z. Phys. C **50**, 11 (1991).
[26] E687 Collaboration, P. L. Frabetti *et al.*, Phys. Lett. B **281**, 167 (1992).
[27] OMEGA Collaboration, M. Adamovich *et al.*, Phys. Lett. B **280**, 163 (1992).
[28] E687 Collaboration, P. L. Frabetti *et al.*, Phys. Lett. B **321**, 295 (1994).
[29] E400 Collaboration, J. P. Cumalat *et al.*, Phys. Lett. B **210**, 253 (1988).